Generation of a poor prognostic chronic lymphocytic leukemia-like disease model: PKCα subversion induces up-regulation of PKCβII expression in B lymphocytes

Rinako Nakagawa,[1,2]* Milica Vukovic,[1,3]* Anuradha Tarafdar,[1] Emilio Cosimo,[1] Karen Dunn,[1] Alison M. McCaig,[1] Ailsa Holroyd,[1] Fabienne McClanahan,[4] Alan G. Ramsay,[5] John G. Gribben,[4] and Alison M. Michie[1]

[1]Institute of Cancer Sciences, College of Medical, Veterinary & Life Sciences, University of Glasgow; [2]The Babraham Institute, Cambridge; [3]MRC Centre for Regenerative Medicine, University of Edinburgh; [4]Centre for Haemato-Oncology, Barts Cancer Institute, Queen Mary University of London; and [5]Department of Haemato-Oncology, King's College London, UK

RN and MV contributed equally to this manuscript.

ABSTRACT

Overwhelming evidence identifies the microenvironment as a critical factor in the development and progression of chronic lymphocytic leukemia, underlining the importance of developing suitable translational models to study the pathogenesis of the disease. We previously established that stable expression of kinase dead protein kinase C alpha in hematopoietic progenitor cells resulted in the development of a chronic lymphocytic leukemia-like disease in mice. Here we demonstrate that this chronic lymphocytic leukemia model resembles the more aggressive subset of chronic lymphocytic leukemia, expressing predominantly unmutated immunoglobulin heavy chain genes, with upregulated tyrosine kinase ZAP-70 expression and elevated ERK-MAPK-mTor signaling, resulting in enhanced proliferation and increased tumor load in lymphoid organs. Reduced function of PKCα leads to an up-regulation of PKCβII expression, which is also associated with a poor prognostic subset of human chronic lymphocytic leukemia samples. Treatment of chronic lymphocytic leukemia-like cells with the selective PKCβ inhibitor enzastaurin caused cell cycle arrest and apoptosis both *in vitro* and *in vivo*, and a reduction in the leukemic burden *in vivo*. These results demonstrate the importance of PKCβII in chronic lymphocytic leukemia-like disease progression and suggest a role for PKCα subversion in creating permissive conditions for leukemogenesis.

Introduction

Chronic lymphocytic leukemia (CLL) is the most common leukemia in the Western world and is characterized by the presence of long-lived mature B cells with the distinct phenotype $CD19^+CD5^+CD23^+IgM^{lo}FMC7^-$.[1] Although deregulation of anti-apoptotic Bcl-2 family members indicates that CLL develops due to inappropriate accumulation of monoclonal B cells,[1,2] assessment of cell turnover reveals that CLL cells also undergo enhanced cell division within proliferation centers of lymphoid organs. This occurs through CLL cell interaction with the stromal niche, antigen and co-stimulation by activated $CD4^+$ T lymphocytes expressing CD40 ligand (CD40L), and interleukin (IL)-4.[3-5] CLL is, therefore, a dynamic disease with significant rates of proliferation and death and complex *in vitro* and *in vivo* disease model systems are required to gain a fundamental understanding of the disease and design suitable therapies.

Clinically, CLL is a heterogeneous disease that can follow an indolent or aggressive course. Over the past decade it has been established that two major prognostic subtypes of CLL can be defined by the mutational status of the variable region of the immunoglobulin heavy chain gene (*IGVH*). Favorable outcomes are associated with the expression of mutated *IGVH* genes, while cases harboring unmutated *IGVH* genes, which can also express the tyrosine kinase, zeta-associated protein 70 (ZAP-70) and CD38, display more aggressive disease and more frequently require therapeutic intervention.[6,7] ZAP-70 expression correlates strongly with unmutated *IGVH*.[8]

While a wealth of research into the biology of CLL has shown the importance of a number of proteins, particularly those assisting in chemoresistance (eg., Mcl-1, absence of p53), no single genetic event has been linked to the initiation of CLL. Due to the heterogeneity within CLL, it is likely that a number of *in vitro* and *in vivo* models will be required to elucidate different aspects of the disease and gain a fuller understanding of the initiation, maintenance and progression of CLL. We previously demonstrated that retroviral-transduction of hematopoietic progenitor cells (HPC) with a kinase dead PKCα construct (PKCα-KR) and subsequent culture either in an *in vitro* B-cell generation culture (OP9 co-culture) or *in vivo* resulted in the generation of CLL-like cells and disease,[9] indicating that modulation of PKCα function may play a role in CLL cell development. In the present study, we further characterize the disease generated upon expression of PKCα-KR in HPC and demonstrate that the CLL-like disease phenotypically resembles poor prognosis CLL.[1] Dissemination of CLL-like cells occurred in lymphoid organs with abnormal distribution in the spleens, and increased CLL-like cells in lymphoid organs, compared with control HPC. In addition, the CLL-like cells had undergone limited/no somatic hypermutation in *IGVH* genes and exhibited up-regulation of ZAP-70 expression and PKCβII expression accompanying

 doi:10.3324/haematol.2014.112276
The online version of this article has a Supplementary Appendix.
Manuscript received on June 12, 2014. Manuscript accepted on January 21, 2015.
Correspondence: Alison.Michie@glasgow.ac.uk

disease maturation, which may account for the proliferation/survival advantage of these cells.[9] Selective targeting of PKCβ activity with enzastaurin resulted in the induction of cell cycle arrest and apoptosis *in vitro* and *in vivo*.

Methods

Animals and cells

Wild-type ICR and C57BL/6 mice were purchased from Harlan Laboratories Ltd. (Oxon, UK), and recombinase activating gene-1-deficient (RAG-1$^{-/-}$) mice were bred and maintained in-house at the University of Glasgow Central Research Facilities (Glasgow, UK). Splenic cell suspensions were generated from aged TCL-1 mice with manifest leukemia (12-month old Eμ-TCL-1 mice) maintained in the Queen Mary University of London animal facility.[10] Timed-pregnant ICR or C57BL/6 mice were generated and fetal liver extracted at E14. Animals were maintained under standard animal housing conditions in accordance with local and Home Office regulations. Peripheral blood samples were obtained, after informed consent, from patients with a clinically confirmed diagnosis of CLL (*Online Supplementary Table S1*). The studies were approved by the West of Scotland Research Ethics Service, NHS Greater Glasgow and Clyde, UK. CLL lymphocytes were isolated as previously described.[11] Normal peripheral blood samples were obtained, after informed consent, from buffy coats of healthy donors and B lymphocytes were separated with MACS human CD19 MicroBeads (Miltenyi Biotec Ltd., Surrey, UK). Leukemic B cells were purified from mouse spleens with MACS mouse CD19 MicroBeads (Miltenyi Biotec Ltd.). GP+E.86 packaging cells produce retrovirus encoding green fluorescent protein (GFP) alone (MIEV-empty vector control) or dominant negative PKCα (PKCα-KR).[12]

In vitro *or* in vivo *B-cell generation*

HPC isolated from E14 fetal liver were prepared and retrovirally-transduced as described previously.[13] Retrovirally-transduced HPC were cultured on a layer of OP9 cells for B-cell development in the presence of IL-7 (Peprotech EC Ltd., London, UK), or adoptively transferred as described previously.[13] Mice were sacrificed between 5 to 8 weeks after injection and the bone marrow, spleen, lymph nodes and blood were collected for analyses.

Flow cytometric analysis

Antibodies were purchased from BD Biosciences (Oxford, UK) unless otherwise stated. Biotin-conjugated antibodies were detected by streptavidin-Pacific blue (Invitrogen, Paisley, UK). Single cell suspensions were prepared and stained as described previously.[13] The cells were acquired on a FACSCantoII (BD Biosciences) using the FACSDiva software package (BD Biosciences) and FlowJo software package (Tree Star Inc, Ashland, OR, USA) to analyze the data. All data shown were lymphocyte-gated by size and hematopoietic lineage gated by CD45^{+} cells. Detailed methods are available in the *Online Supplement*.

Histology and immunohistochemistry

Spleens were collected from HPC-reconstituted mice and control RAG-1$^{-/-}$ mice after 5 weeks and fixed in neutral buffered formalin (Sigma-Aldrich) at 4°C overnight and embedded in paraffin following a standard ethanol and xylene protocol. Tissue sections were scanned with the SlidePath Digital Pathology Solutions system (Leica Microsystems Ltd., Milton Keynes, UK). Detailed methods are available in the *Online Supplement*.

Cell cycle, apoptosis and proliferation analysis

Cell cycle was analyzed by detecting DNA content, visualized with propidium iodide (PI) intercalation as described previously.[9] A BrdU incorporation assay was performed using the Cell Proliferation Elisa BrdU kit (Roche Diagnostics, West Sussex, UK), following the manufacturer's protocol. Apoptosis was determined by analyzing annexin V/DAPI staining (BD Biosciences), as previously described.[14]

Determination of the mutational status of IGVH

C57BL/6 fetal liver-derived HPC were prepared, retrovirally-transduced and transferred into RAG-1$^{-/-}$ mice with C57BL/6-derived thymocytes. Mice were sacrificed at 5 weeks after injection. GFP^{+} splenic cells were isolated by cell sorting on a FACSAriaI (BD Biosciences), RNA was extracted using an RNAeasy kit (Qiagen, Manchester, UK) and reverse transcribed with AMV (Roche Diagnostics) using oligo(dT)15 primers. cDNA was amplified with PCR primer combinations and cycles described elsewhere.[15] Successfully amplified PCR products were cloned into pCRII-Blunt-TOPO (Invitrogen) and sequenced with M13 reverse/forward primers. The data acquired were analyzed using IMGT (*www.imgt.org*).

Western blots

MIEV- or PKCα-KR-HPC co-cultures were removed from the OP9 layer and placed on plastic in complete medium for 2 h in order to separate cells from adherent OP9 cells. Lysates containing equal amounts of protein were separated by sodium dodecylsulfate-polyacrylamide gel electrophoresis, transferred onto polyvinyl difluoride membrane, and blocked as described previously.[16] All antibodies were obtained from Cell Signaling Technologies (Danvers, MA, USA) except anti-PKCβ$_{I}$ (E-3) and anti-PKCβ$_{II}$ (sc-210) antibodies, which were obtained from Santa Cruz Biotechnology (Santa Cruz, CA, USA). The blots were developed with an Immun-Star™ Western C™ HRP chemiluminescence kit, and imaged with the Molecular Imager® ChemiDoc™ XRS system (Bio-Rad Laboratories, Hempstead, UK).

Quantitative real-time polymerase chain reaction

Quantitative real-time polymerase chain reaction (PCR) was performed in triplicate with the 7900HT Fast Real-Time PCR system (Applied Biosystems, Warrington, UK) using the Taqman® Gene Expression Assay probe and primer set, and analyzed on the ABI Prism 7900HT (Applied Biosystems) for mouse *prkcb* and *aicda*, with *gapdh* was used as a reference gene, as described previously.[16]

In vitro *and* in vivo *drug treatment*

In vitro MIEV- or PKCα-KR-HPC co-cultures were removed from the OP9 layer and density-centrifuged with Lympholyte-Mammal to remove dead cells. One million cells were cultured in the presence of IL-7 (10 ng/mL) and treated with enzastaurin (LY317615, a kind gift from Eli Lilly) at the indicated concentrations. Dimethyl sulfoxide (DMSO) was added as a vehicle, no-drug control. For *in vivo* studies, CLL-like disease was generated in mice as described above. Mice with confirmed leukemia (≥ 0.4% GFP^{+}CD19^{+} in the blood) were treated 4 – 6 weeks after injection with 75 mg/kg enzastaurin or vehicle (5% dextrose in water), twice a day for up to 21 days by oral gavage and then sacrificed for analyses.

Results

Infiltration of chronic lymphocytic leukemia-like cells in the lymphoid organs of mice adoptively transferred with PKCα-KR-expressing hematopoietic progenitor cells

We have previously shown that PKCα-KR expression in

wild-type mouse HPC, and subsequent culture in an *in vitro* B-cell generating environment (HPC-OP9 co-culture) leads to the generation of a population of cells phenotypically similar to human CLL ($CD19^+CD23^+CD5^+sIgM^{lo}$; Figure 1A[9]). During the *in vitro* development of B cells, up-regulation of the mature B lineage marker CD23 was evident on both MIEV- and PKCα-KR-expressing cells by day (d) 10 of co-culture, with significantly higher expression noted on PKCα-KR-expressing cells (Figure 1B). CD23 expression was not accompanied by IgM up-regulation, but was instead associated with higher expression of CD5 in PKCα-KR-expressing cells (Figure 1C). Moreover, the percentage of the $CD19^+CD5^+$ population increased significantly during the PKCα-KR cultures, while remaining unchanged in the MIEV cultures (*Online Supplementary Figure S1*).

Reconstitution of mice with an increasing number of PKCα-KR-HPC ($1x10^5$, $3x10^5$, $5x10^5$) significantly reduced mouse survival, with the majority of mice succumbing to a CLL-like disease between 6 – 9 weeks when reconstituted with $3x10^5$ PKCα-KR-HPC. As expected, reconstitution of mice with $5x10^5$ MIEV-HPC did not affect survival (Figure 2A). Analysis of spleen size suggested an increase in cell number in PKCα-KR-HPC-reconstituted mice, due to an increase in spleen weight compared with that in MIEV-HPC and $RAG^{-/-}$ mice (Figure 2B). Analysis of the splenic architecture from MIEV- or PKCα-KR-HPC-reconstituted mice revealed the development of lymphoid fol-

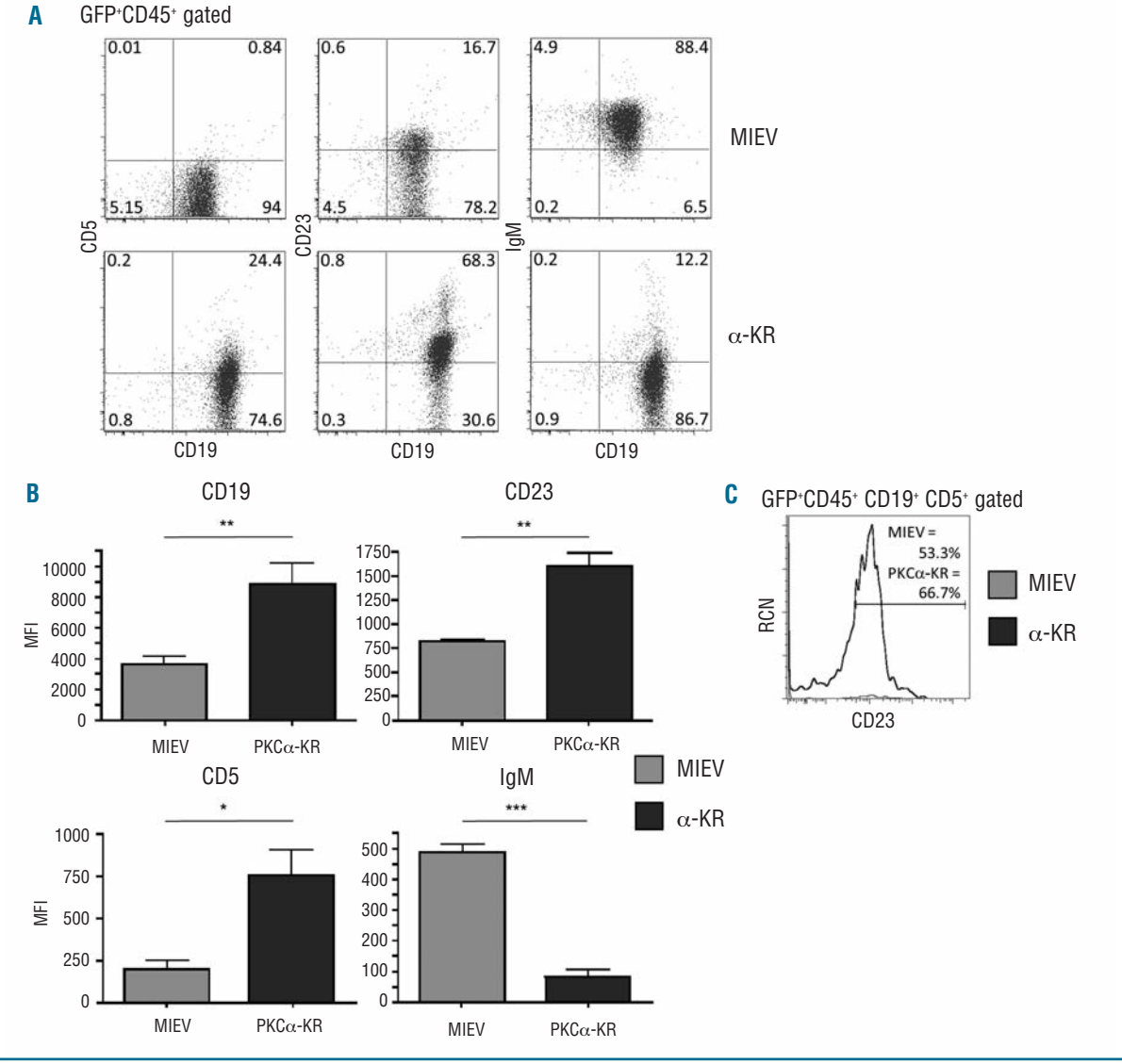

Figure 1. PKCα-KR-expressing cells phenotypically resemble human CLL cells according to surface protein expression. (A) MIEV- or PKCα-KR-HPC-OP9 co-cultures were analyzed by flow cytometry at d10. FACS plots shown are live- and size- (FSC/SSC) and hemopoietic lineage ($CD45^+$)-gated prior to analysis for CD5 *vs.* CD19, CD23 *vs.* CD19 and IgM *vs.* CD19 as indicated. Percentages are indicated in the corner of the quadrants. (B) The mean fluorescence intensity (MFI) of CD19, CD5, CD23 and IgM was calculated for a minimum of three individual biological replicates. Data are presented as mean (± SEM). *P* values were generated using a Student unpaired t-test to compare groups (**P*<0.05; ***P*<0.005; ****P*<0.001). (C) A histogram comparing the surface expression of CD23 on $GFP^+CD45^+CD19^+CD5^+$-gated MIEV or PKCα-KR cells, against relative cell number (RCN).

licular structures that were absent from the RAG$^{-/-}$ host spleen (Figure 2C). However PKCα-KR follicular cells were unusually distributed resulting in a disorganized splenic architecture, as indicated by H&E staining of splenic sections and immunohistochemistry staining for the B lineage marker B220, which co-stains with CD19^{+} cells in both MIEV- and PKCα-KR-transduced cells (Figure 2C, *Online Supplementary Figure S2*). H&E staining also revealed lymphocyte infiltration in the liver of PKCα-KR mice, but not MIEV mice (*Online Supplementary Figure S3*). Flow cytometric analyses of retrovirally-transduced GFP^{+} cells that populate the lymphoid organs of reconstituted mice revealed a small population of GFP^{+}CD19^{+}CD5^{-} B lineage cells in the bone marrow, spleen and blood of MIEV-HPC mice. However, in PKCα-KR-HPC mouse organs and blood, the majority of CD19^{+} B cells were CD5^{+}, similar to CLL cells (Figure 2D,E). The percentage of GFP^{+}CD19^{+}CD5^{+} B cells detected in blood, spleen, bone marrow and lymph nodes was significantly higher in PKCα-KR-mice than in GFP^{+}CD19^{+} MIEV control mice (Figure 2E). Moreover, the GFP^{+}CD19^{+}CD5^{+} B-cell population was detectable in blood at 3 weeks and increased over time (*Online Supplementary Figure S4*).

PKCα-KR transduced cells exhibit features of the poor prognostic subgroup of chronic lymphocytic leukemia patients

Examination of ZAP-70 expression levels in *in vitro*-gen-

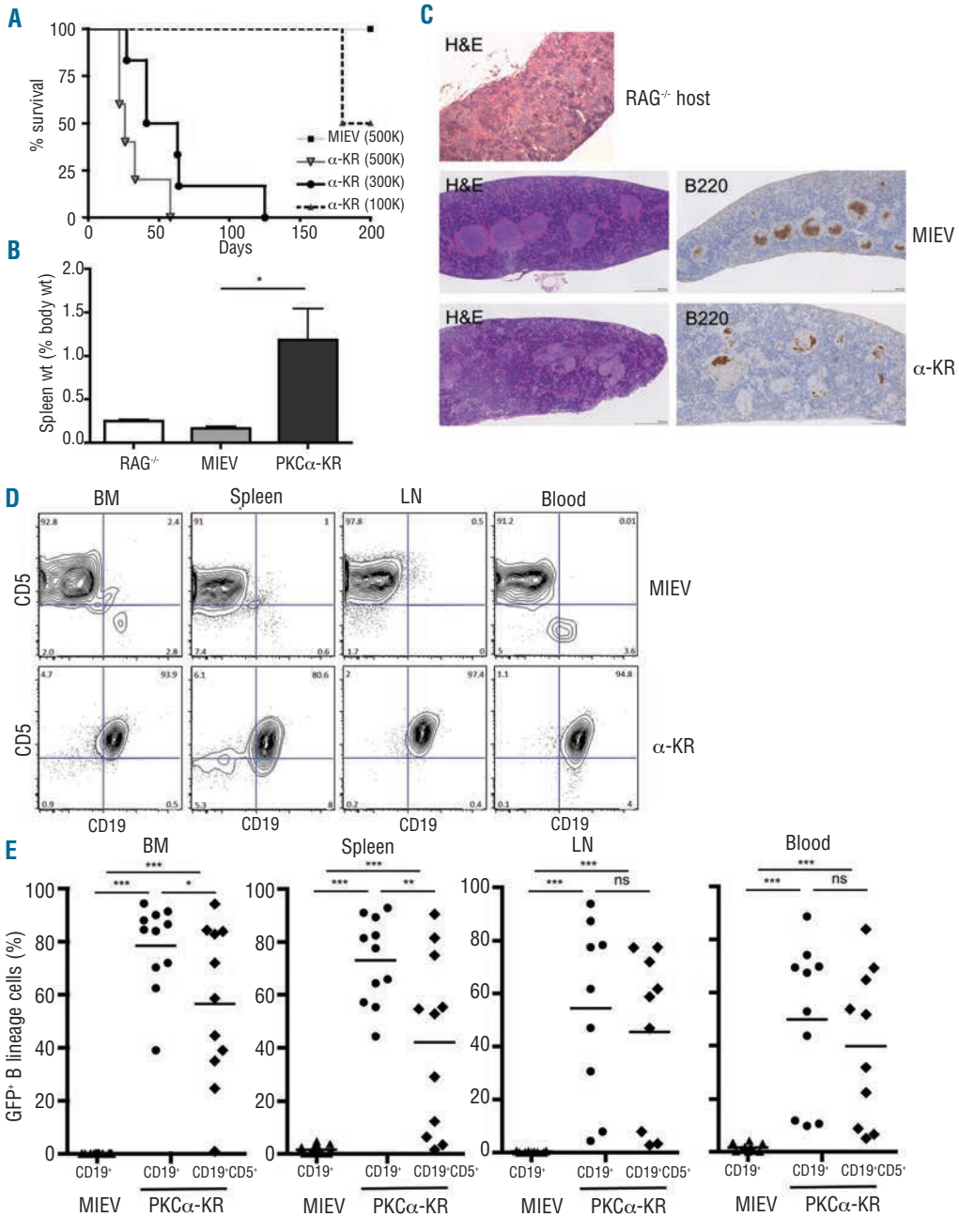

Figure 2. CLL-like cells disseminate into primary and secondary lymphoid organs. MIEV- and PKCα-KR-HPCs were injected (i.p.) into RAG-1$^{-/-}$ neonates. (A) Kaplan-Meier curves comparing the survival rates in mice adoptively-transferred with MIEV-HPCs [500K-pale gray line, square (n=5) or PKCα-KR-HPC (500K-mid-gray line, triangle (n=5); 300K-dark gray line, circle (n=6); 100K-dotted line (n=4)]. Log-rank (Mantel-Cox) test showed an overall significant difference (P=0.0013). The log-rank test of trend revealed a significant linear trend between the number of cells injected and the survival of mice (P=0.0001). (B) Spleen weights from RAG$^{-/-}$, MIEV-HPC and PKCα-KR-HPC mice are shown as a percentage of total body weight. A Student unpaired t-test was performed; *P<0.05. The graphs were generated from six spleens per condition. (C) Five-week post-reconstitution mice were sacrificed. Paraffin-embedded spleens from RAG$^{-/-}$ host mice (top) MIEV (middle) or PKCα-KR (bottom) were sectioned and stained with either H&E (left) or anti-B220 antibody (brown; right); 40 x magnification shown. (D) Single cell suspensions were prepared from organs as indicated and analyzed by flow cytometry for CLL cell markers, CD19 and CD5 after live- and size-(FSC/SSC) and GFP^{+}CD45^{+} gating. (E) The percentage of GFP^{+}CD19^{+} cells or GFP^{+}CD19^{+}CD5^{+} cells within total hematopoietic CD45^{+} cells in the indicated organs is shown for mice reconstituted with MIEV- or PKCα-KR-HPC as indicated. A Student unpaired t-test was performed; *P<0.05, **P<0.005, ***P<0.001. The graphs were generated using data from ten individual mice.

erated CD19+ B cells and splenic B cells isolated from PKCα-KR-HPC mice by flow cytometry revealed that PKCα-KR-expressing cells up-regulated ZAP-70 expression compared to control B cells and the established CLL mouse model Eμ-TCL-1 (Figure 3A,B). Low level ZAP-70 expression is observed in MIEV-expressing cells, which has previously been described in normal mature B cells (Figure 3A[17]). Analysis of *IGVH* mutational status revealed that the majority of PKCα-KR-expressing cells isolated from spleens had unmutated *IGVH* genes (6/8 sequences), compared with half (4/8 sequences) of the MIEV-expressing cells (Table 1). Interestingly, the *IGVH* genes contained longer CDR3 regions in PKCα-KR-expressing cells. Western blotting analysis revealed an activation of the ERK-MAPK and mTorc-1 pathways, as indicated by elevated phosphorylation of ERK1/2 and S6 in PKCα-KR cells (Figure 3C). Prolonged activation of the MEK/ERK pathway is associated with anti-apoptotic characteristics of CLL cells.[18] PKCα-KR cells also exhibited an elevated proliferative capacity compared with control B cells, both *in vitro* and *in vivo* (Figure 3D,E). Supporting this, *aicda* expression, which has been associated with increased CLL cell proliferation,[19,20] was significantly increased in GFP+CD19+ cells expressing PKCα-KR at the later stages of culture compared to MIEV-expressing cells (Figure 3F).

We previously demonstrated that PKCα-KR-transduced cells exhibited reduced PKC activity during the early stages of the OP9 co-culture, as expected (Figure 4A, left).[9] However we observed an elevation in PKC activity later in the co-cultures, at d17 (Figure 4A, right and 4B). As PKCβII up-regulation has previously been associated with poor prognosis in CLL patients, we analyzed PKCβ expres-

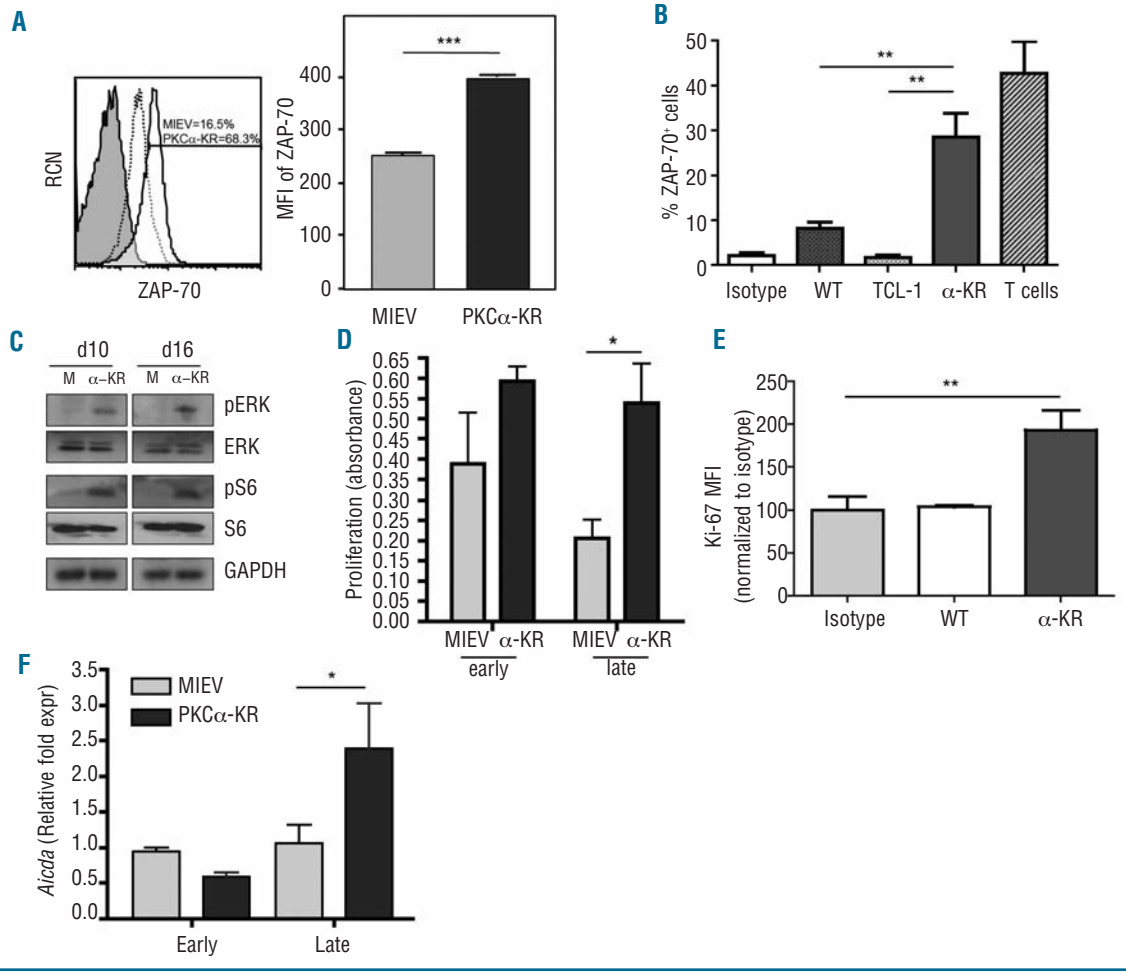

Figure 3. PKCα-KR-transduced CLL-like cells resemble poor prognostic CLL patients' samples. (A) MIEV- or PKCα-KR-HPC were analyzed by flow cytometry for intracellular levels of ZAP-70 at d12 of co-culture. Solid line, PKCα-KR; dotted line, MIEV; shaded, isotype control. A representative blot of three independent cultures is shown. (B) The percentage of ZAP-70+ cells was analyzed by flow cytometry in B lineage cells isolated from the spleens of ICR-WT, Eμ-TCL-1 Tg and PKCα-KR-HPC mice. Isotype control and ICR-T-cell-positive control are shown. (C) Protein lysates were prepared from MIEV-FL or PKCα-KR-FL co-cultures at d10 and d16. Western blots were carried out, immunoblotting for phosphorylated and total ERK1/2, phosphorylated and total S6, and an additional loading control, GAPDH. (D) Proliferation was assessed by culturing 50,000 MIEV- or PKCα-KR cells from early (d6 – d10) and late (d15 – d20) stages of the cultures and incubating cells with BrdU for 2 h prior to the end of the 24 h timepoint. Data are represented as mean (± SEM) of at least three biological replicates, each carried out in technical triplicates. (E) Ki-67 expression levels (MFI) were analyzed in CD19-MACS-purified ICR-WT and PKCα-KR-HPC spleens. (F) RNA was isolated from MIEV- or PKCα-KR-OP9 cells derived from early (d6 – d10) and late (d15 – d20) stages of the cultures and subjected to quantitative reverse transcription-PCR to evaluate the levels of *aicda* expression. Results are expressed as $2^{(-\Delta\Delta CT)}$ relative to the *GAPDH* reference gene. Data are represented as mean (± SEM) of at least three biological replicates, each carried out in technical triplicates. A Student unpaired t-test was performed; **P*<0.05, ** *P*<0.005.

sion.[21] Analysis of PKCα-KR-transduced cells revealed up-regulation of both *prkcb* expression (*Online Supplementary Figure S5*) and PKCβII protein expression in PKCα-KR-transduced cells compared with the levels in MIEV control cells, while PKCβI expression was unaltered (Figure 4C).

To determine the stage at which PKCβII is up-regulated during the development of CLL-like cells on OP9 co-culture, MIEV- or PKCα-KR co-cultures were harvested as indicated and PKCβII expression was determined. PKCβII expression increased between d10 and d15 of co-culture in PKCα-KR-transduced cells, while remaining unchanged in MIEV control cells (Figure 4D). Up-regulation of PKCβII and concomitant down-regulation of PKCα expression has previously been shown in CLL patients' samples,[21,22] a finding that was confirmed in our CLL cohort. Compared to PKCα expression in peripheral blood B lymphocytes obtained from healthy volunteers, PKCα was barely detectable in the majority of CLL samples (12/16 samples), while PKCβII expression was elevated in half of the samples assessed (Figure 4E). Analysis of this cohort did not indicate an association of absent/low PKCα expression with a specific prognostic subgroup of CLL patients (*Online Supplementary Table S1*). PKCα expression was down-regulated in B cells isolated from Eμ-TCL-1 spleens compared with the expression in age-matched, wild-type controls; the difference did not, however, reach statistical significance (Figure 4F). Interestingly PKCα expression was also down-regulated in PKCα-KR-expressing splenic B cells. There was a trend towards up-regulation of PKCβII expression in *in vivo*-generated PKCα-KR B cells but not in purified Eμ-TCL-1 splenic B cells, which exhibited similar PKCβII expression to that of age-matched, control B cells (Figure 4F). Analysis of the ERK-MAPK-mTor signaling pathway *in vivo* demonstrated a significant activation of mTor kinase, as indicated by the elevation in phosphorylated S6 both in PKCα-KR-expressing and Eμ-TCL-1 splenic B cells (Figure 4G). However, pERK exhibited variability between mice and so there was not a clear up-regulation of ERK-MAPK activity.

Our CLL-like cells exhibit a higher expression of markers associated with adverse outcome in CLL patients and possess an enhanced proliferation capacity, likely due to elevated mTor signaling upon PKCα subversion. This, coupled with the finding that PKCα expression is reduced in the majority of CLL patients' samples assessed, indicates that our CLL-like disease model is a translationally-relevant model for the progressive human disease.

PKCβ selective inhibitors inhibit chronic lymphocytic leukemia-like cell proliferation in vitro *and* in vivo

To determine whether PKCβ plays an important role in driving proliferation and cell survival in our mouse CLL-like disease model *in vitro*, CLL-like cells were treated with the PKCβ selective inhibitor, enzastaurin. PKCβ has previously been shown to phosphorylate and inhibit GSK3β.[23] Therefore, to test the selectivity of enzastaurin for PKCβ-mediated signals, we assessed the phosphorylation status of GSK3β. PKCα-KR-expressing cells from late co-cultures exhibited increased phospho-GSK3β[S9], an effect that was abrogated by enzastaurin treatment (20 μM; Figure 5A). Enzastaurin treatment induced a selective and significant elevation in apoptosis above background both in PKCα-KR-expressing cells (left) and splenic Eμ-TCL-1 cells (right) compared with control cells, as indicated by an elevation in the percentage of annexin V^+DAPI^- cells among the leukemic cells (Figure 5B, *Online Supplementary Figure S6*).

Analysis of the effect of enzastaurin treatment on cellular proliferation revealed a G1 arrest in PKCα-KR-cultures only (Figure 5C, left). This was accompanied by a significant reduction in the proportion of cells undergoing mitosis in PKCα-KR-cultures (Figure 5C, right). Coupled with

Table 1. Summary of *IGVH* rearrangements generated in mice transplanted with MIEV- or PKCα-KR-expressing cells. GFP^+ leukemic B cells generated *in vivo* were isolated prior to cloning and sequencing of *IGVH* regions. Sequences were analyzed using IMGT (*www.imgt.org*). In-frame sequences are shown.

Sample N.	V_H gene	J_H gene	D_H gene	Similarity to germline (%)	Mutational status	CDR3 length
MIEV-1	IGHV1-9*01	IGHJ4*01	IGHD2-3*01	99.7	UM	14
MIEV-2	IGHV1S20*02	IGHJ2*01	IGFD1-1*01	98.6	UM	11
MIEV-3	IGHV1S132*01	IGFJ4*01	IGHD1-1*02	98.6	UM	13
MIEV-4	IGV5-4*02	IGHJ3*01	IGHD4-1*01	97.1	M	11
MIEV-5	IGHV1S15*01	IGHJ3*01	IGHD2-3*01	98.3	UM	9
MIEV-6	IGHV14-1*01	IGHJ3*01	IGHD2-12*01	97.1	M	13
MIEV-7	IGHV1-63*02	IGHJ1*01	IGHD2-1*01	97.1	M	11
MIEV-8	IGHV1-9*01	IGHJ4*01	IGHD2-3*01	97.6	M	14
PKCα-KR-1	IGHV1-39*01	IGHJ4*01	IGHD2-1*01	98.6	UM	12
PKCα-KR-2	IGV1S20*02	IGHJ2*01	IGHD1-1*01	93.3	M	14
PKCα-KR-3	IGHV1-63*02	IGHJ4*01	IGHD3-2*02	97.1	M	14
PKCα-KR-4	IGHV1-39*01	IGHJ4*01	IGHD2-1*01	100	UM	12
PKCα-KR-5	IGHV1-69*02	IGHJ1*03	IGHD1-1*01	98.9	UM	16
PKCα-KR-6	IGHV1-23*01	IGHJ1*01	IGHD1-1*01	99.3	UM	13
PKCα-KR-7	IGHV14-4*01	IGHJ3*01	IGHD1-1*01	99	UM	14
PKCα-KR-8	IGHV81*01	IGHJ2*01	IGHD2-1*01	99	UM	13

M: mutated; UM: unmutated.

these data, enzastaurin treatment significantly reduced the BrdU incorporation of PKCα-KR cells at 24 and 48 h (Figure 5D). In addition, and supporting the data presented in Figure 3D, PKCα-KR-expressing cells exhibited a significantly higher proliferation rate than MIEV cells in untreated cultures, and treatment of these cells with enzastaurin reduced their proliferation rate to that of MIEV cells (Figure 5D). These results demonstrate that enzastaurin selectively inhibited cell cycle progression and proliferation in CLL-like cells *in vitro*.

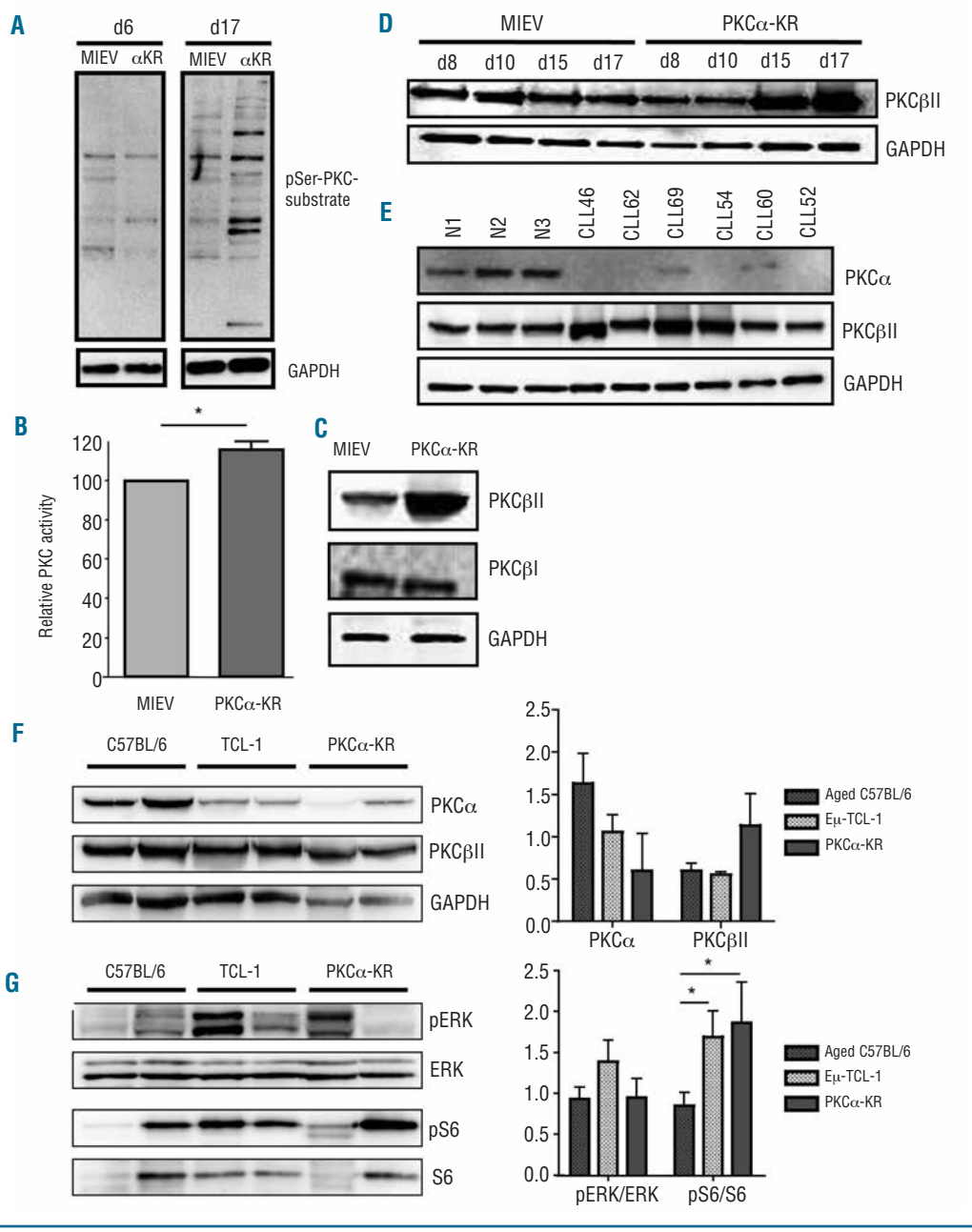

Figure 4. CLL cells isolated from mouse models and CLL patients samples exhibit altered PKC isoform expression profiles. (A) Protein lysates were prepared from MIEV- or PKCα-KR-HPC derived cells at the indicated times, separated by gel electrophoresis and immunoblotted for PKC substrates using the anti-phospho-Ser PKC substrate antibody (pSer-PKC-substrate). GAPDH was included as a protein loading control. (B) Protein kinase assay was carried out on cells prepared from d17 MIEV- or PKCα-KR-OP9 co-cultures. A Student unpaired t-test was performed; **P*<0.05. (C) Protein lysates were prepared from MIEV- or PKCα-KR-OP9 co-cultures and immunoblotted for PKCβI, PKCβII and GAPDH as a protein loading control. (D) Protein lysates were prepared from earlier and later MIEV- or PKCα-KR-OP9 co-cultures as indicated and immunoblotted for PKCβII and GAPDH as a protein loading control. (E) Protein lysates were prepared from B lineage cells of freshly isolated peripheral blood samples derived from healthy donors or CLL patients. Membranes were immunoblotted for PKCα, PKCβII and GAPDH as a protein loading control. (F) Protein lysates were prepared from MACS-isolated spleen B cells from age-matched C57BL/6 (n=5), Eμ-TCL-1 Tg (n=5) and PKCα-KR-expressing (n=4) mice and immunoblotted for PKCα, PKCβII and GAPDH as a protein loading control. A representative blot (left) and the mean expression (±SEM) of PKCα (left) and PKCβII (right) as a ratio of GAPDH are shown. (G) Protein lysates were prepared from MACS-isolated spleen B cells of Eμ-TCL-1 Tg (n=5), PKCα-KR-expressing (n=4) and age-matched C57BL/6 (n=5) mice and immunoblotted for pERK/ERK and pS6/S6. A representative blot (left) and the mean expression (±SEM) of pERK as a ratio of ERK (left) and pS6 as a ratio of S6 (right) are shown.

To test the efficacy of enzastaurin at inhibiting proliferation of CLL-like cells *in vivo*, mice were treated with enzastaurin twice a day for up to 3 weeks, after confirmation that the mice were leukemic (≥0.4% GFP$^+$CD19$^+$CD5$^+$ cells in the blood). Enzastaurin-treated mice displayed a decrease in the percentage and number of GFP$^+$CD19$^+$CD5$^+$ cells in the bone marrow, spleen, lymph nodes and blood compared with vehicle-treated controls, with the differences reaching significance in the bone marrow, spleen and blood (Figure 6A-C). Interestingly, a decrease in CLL-like cells in the blood was observed during treatment, although this did not reach statistical significance. In addition, there was a significant induction of apoptosis in enzastaurin-treated CLL-like cells in both the bone marrow and spleen, compared with the apoptosis of vehicle-treated CLL cells (Figure 6D). Collectively, these results indicate that targeted therapies towards PKCβ-mediated signaling pathways show promise as potential therapies for progressive CLL, by impeding CLL cell proliferation and inducing apoptosis.

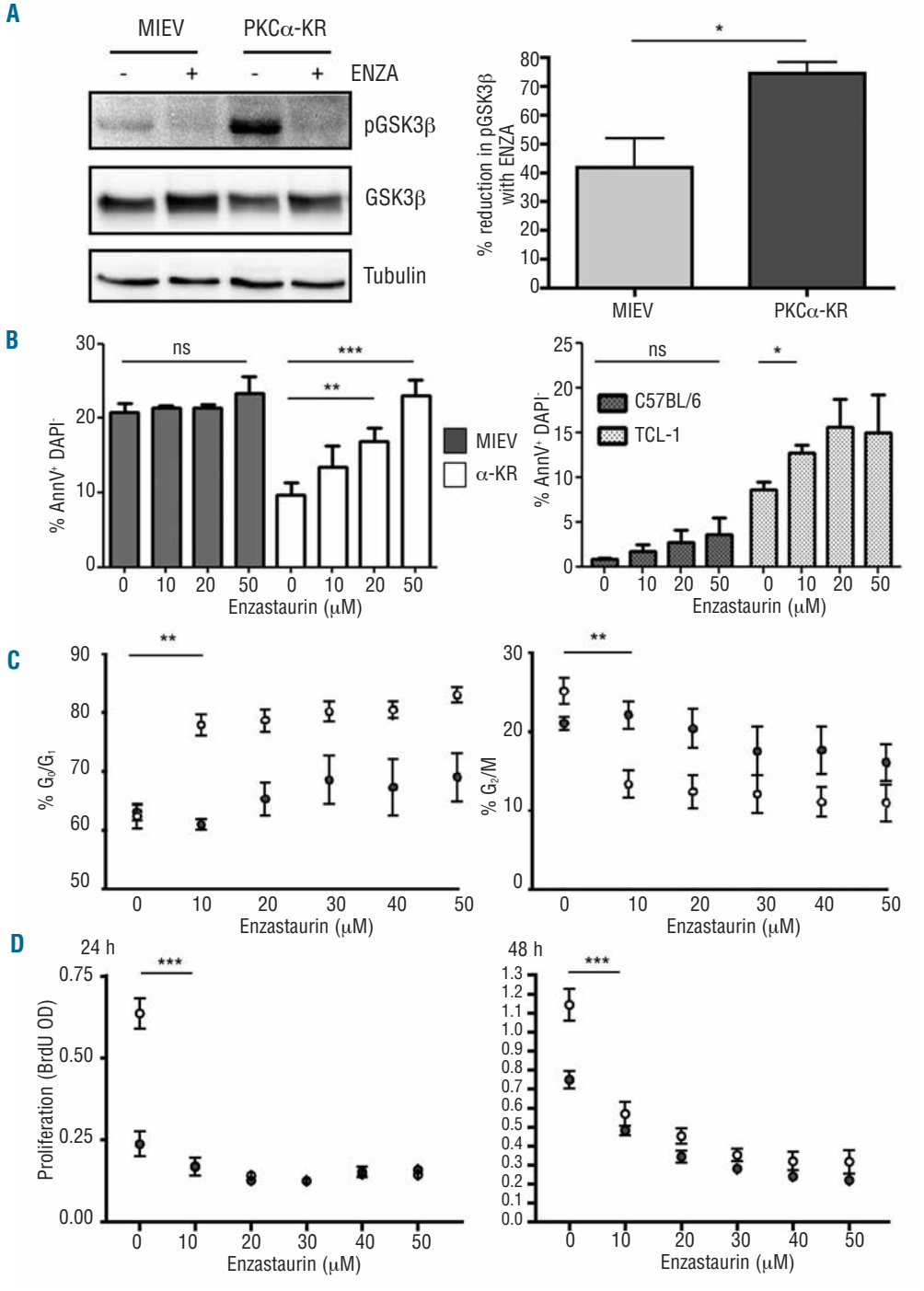

Figure 5. Enzastaurin induced cell cycle arrest and apoptosis in CLL-like cells. MIEV- or PKCα-KR-HPC-derived cells were cultured for 24 hr in the presence of enzastaurin (ENZA) as indicated. (A) Protein lysates were prepared from late co-cultures (post-d15) of MIEV- or PKCα-KR-expressing cells. Proteins separated by gel electrophoresis and immunoblotted for phospho-GSK3β^{S9}, GSK3β and tubulin as a protein loading control. Densitometry was performed on the blots, assessing the phospho-GSK3β^{S9} signal compared with GSK3β signal strength. The mean percentage (± SEM) of phospho-GSK3β signal reduction from untreated cells in three independent experiments is shown. (B) Flow cytometry was used to assess the level of apoptosis induced by enzastaurin treatment of MIEV- *vs.* PKCα-KR cells and splenic B lineage cells isolated from age-matched C57BL/6 *vs.* Eμ-TCL-1 transgenic mice. Annexin V$^+$DAPI$^-$ cells represent early apoptotic cells. Data are represented as mean (± SEM) of three biological replicates. (C) PI analysis was used to calculate the phases of the cell cycle (G_0/G_1 and G_2M shown). Data shown exclude the sub-G_0 population. Data are represented as mean (± SEM) of at least three biological replicates. Open circle (○) PKCα-KR; filled circle (●) MIEV. (D) MIEV- or PKCα-KR-expressing cells were cultured for 24 or 48 h in the presence of ENZA, as indicated. Cells were incubated with BrdU for 2 h prior to the end of the timepoint. Absorbance values were read at 492 nm to 370 nm after addition of TMB substrate. Data shown are the mean (± SEM) of at least three biological replicates, each carried out in technical triplicates. *P* values were generated using the Student unpaired t-test **P*<0.05, ***P*<0.005, ****P*<0.001.

Discussion

We previously established that subversion of PKCα confers a CLL-like phenotype to B lineage cells both *in vitro* and *in vivo*.[9] We now demonstrate that PKCα-KR-expressing CLL-like cells display poor prognostic features of the human disease both *in vitro* and *in vivo*, and aberrantly expand in lymphoid organs of mice *in vivo*. These CLL-like cells exhibit elevated proliferation, likely due to an activation of ERK-MAPK-mTor signaling, indicating that PKCα-KR-expressing cells display properties of progressive disease. Importantly, we demonstrated that PKCα expression was down-regulated in the majority of CLL cases assessed, indicating that this model is translationally rele-

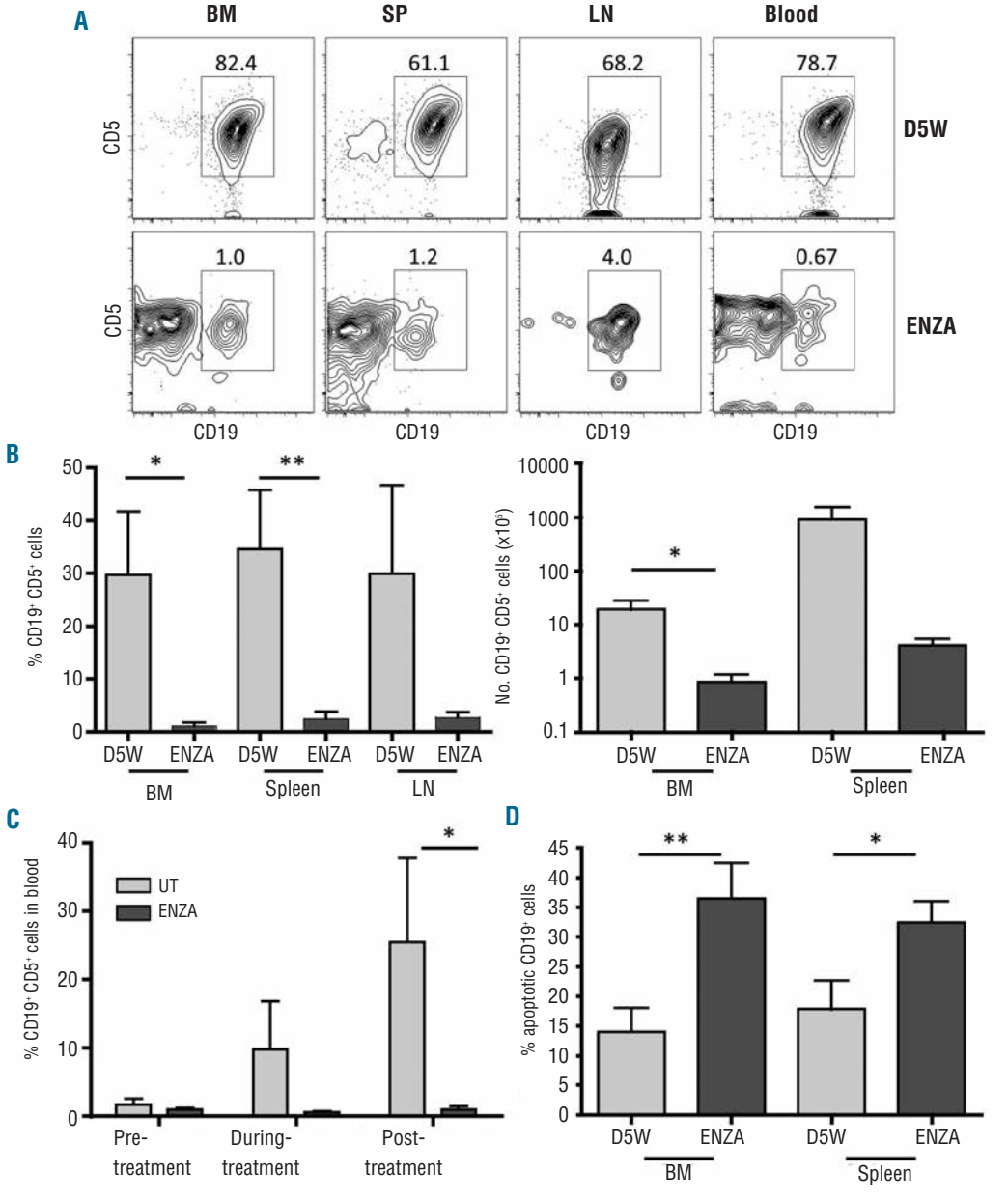

Figure 6. Enzastaurin (ENZA) reduced leukemic burden and selectively induced apoptosis in CLL-like cells *in vivo*. CLL-like diseased mice were generated by adoptively transferring 4x10^5 PKCα-KR-FL cells into RAG-1$^{-/-}$ neonates. Four to six weeks after injection, on confirmation of a population of CLL-like cells in the blood (≥ 0.4%), mice were dosed with either ENZA or vehicle control 5% dextrose in water (D5W) for up to 21 days. Thereafter, blood, bone marrow (BM), spleen (SP) and lymph nodes (LN) were analyzed for leukemic burden and level of apoptosis by flow cytometry as indicated. (A) Representative flow cytometric analysis of vehicle- or ENZA-treated mice. Data shown were analyzed for CLL cell markers, CD19 and CD5 after live- and size- (FSC/SSC), GFP$^+$ and CD45$^+$ gating. The percentage of GFP$^+$ CLL-like cells within the total population is shown. (B) Percentages (left) and numbers (right) of the GFP$^+$CD45$^+$CD19$^+$CD5$^+$ population are shown in the ENZA- and D5W-treated mice in the organs indicated. (C) Percentages of GFP$^+$CD45$^+$CD19$^+$CD5$^+$ cells in the blood before, during, and after ENZA-treatment and vehicle administration. (D) Percentages of annexin V$^+$7-AAD$^-$ apoptosing cells were calculated within the GFP$^+$CD19$^+$ population of ENZA- and vehicle-treated mice. Data shown are the mean (± SEM) of six individual mice. *P* values were generated using the Student unpaired t-test **P*<0.05, ***P*<0.005.

vant for the study of CLL. Subsequent to PKCα-KR expression we identified an elevation in PKCβII expression, a PKC isoform that has been implicated in CLL pathogenesis, which, when inhibited with enzastaurin, reduced tumor load within the spleen, due to the induction of cell cycle arrest and apoptosis.

Expression patterns of specific PKC isoforms are dysregulated in a number of cancers. PKCα is up-regulated in breast, gastric, prostate and brain cancers, suggesting that it contributes to tumorigenesis,[24,25] and higher expression levels have been linked with the aggressiveness and invasive capacity of breast cancer cells.[26,27] However, PKCα expression is down-regulated in epidermal, pancreatic, and colon cancers[28-32] and CLL[21] suggesting that PKCα can also function as a tumor suppressor. This was demonstrated in mouse models for colon cancer, in which a reduction in PKCα expression was observed in carcinogen-induced colon cancer,[32] and $APC^{min/+}$ mice.[33] Indeed, crossing $APC^{min/+}$ mice onto the $PKC\alpha^{-/-}$ background led to an accelerated, more aggressive development of colon cancer.[33,34] Interestingly, spontaneous development of cancerous lesions in the intestinal tract occurred with higher frequency in aging $PKC\alpha^{-/-}$ mice than in littermate controls. The malignant cells within the lesions derived from $PKC\alpha^{-/-}$ mice had a higher mitotic index than that of cells from littermate controls. Taken together, these data strongly suggest a role for PKCα in the regulation of cell division and suppression of tumor formation in selected cancers.[33] Of note, PKCβII up-regulation has been intrinsically linked to the development of colon cancer.[32,35] Similarly, PKCβ has recently been shown to be essential for CLL development in the TCL-1 Tg CLL mouse model, with deletion of PKCβ in a murine model of CLL leading to an increase in survival.[36] Surprisingly, we found that PKCβII expression remained unchanged in B lineage cells isolated from TCL-1 Tg splenic cells; however, a reduction in PKCα expression was observed. Down-regulation of PKCα expression/function may contribute to the development/progression of CLL in both TCL-1 Tg mice and the PKCα-KR mouse model, similar to the effect noted in colon cancer models. Interestingly, PKCα expression was also reduced in the PKCα-KR mouse model, whilst GFP expression was maintained. This finding suggests that PKCα may be post-translationally targeted for degradation in CLL cells, resulting in decreased expression.[37] Results from the *in vitro* co-cultures of our model indicate that up-regulated PKCβII is not required for the initiation of CLL-like cells, as $GFP^{+}CD19^{+}CD5^{+}$ cells were present during the early stages of the cultures, prior to PKCβII up-regulation. These results suggest that loss of PKCα function may create permissive conditions for the generation of CLL, while PKCβII activation/up-regulation enables disease progression. Indeed, the block in CLL development in the $PKC\beta^{-/-}$-TCL-1 Tg model may reflect the absence of both PKCβI and PKCβII in these mice.

Mouse models form an integral part of the pre-clinical development of promising therapies.[38] Due to the heterogeneity of CLL, it is important to generate models that represent the complexity of the disease. For example targeting a component of the 13q deletion incorporating the DLEU gene product in mice, present in over 50% of patients, resulted in the development of CLL.[39] In addition, the development of a CLL phenotype in Eμ-TCL-1 Tg mice resulted in subsequent studies establishing that TCL-1 is preferentially expressed in patients with a poor prognosis.[40,41] Here, we demonstrated that CLL cells express lower levels of PKCα than their normal B-cell counterparts suggesting that reduced expression levels of PKCα may assist in generating permissive conditions for the development of CLL. Like the TCL-1 Tg mouse, our model predominantly expresses unmutated *IGVH* genes that have longer CDR3 regions, a characteristic of subsets of poor prognostic CLL patients.[42,43] In contrast, ZAP-70 is up-regulated in PKCα-KR-expressing CLL-like cells while, as shown previously, it is absent in TCL-1 splenic B cells,[44] which may reflect a difference in the cell of origin between these two models. These findings suggest that the two mouse models provide complementary disease systems for studying the pathogenesis of poor prognostic CLL. Notably, an advantage of the PKCα-KR model over the TCL-1 Tg mouse is the former's rapid and reliable disease onset, in a timeframe of weeks compared to months, which is beneficial when performing *in vivo* drug testing.

Although the molecular basis of CLL has not been fully understood, PKC-mediated signals control CLL survival and proliferation, and thus represent promising therapeutic targets. Enzastaurin has previously been shown to induce apoptosis in CLL cells independently of mutational status in an *in vitro* culture system.[36] Enzastaurin-mediated apoptosis has been reported to be dependent on PP2A activity.[45] Interestingly, inhibition of PKC activity by treating cells with ruboxistaurin (targeting PKCβ) or sotrastaurin (AEB071; a pan-PKC inhibitor) results in the down-regulation of the protein tyrosine kinase PTPN22, which plays a protective role in BCR-mediated CLL survival, leading to apoptosis *in vitro*.[46] Our studies demonstrate a selective induction of apoptosis in leukemic cells and a reduction in cellular proliferation with enzastaurin *in vitro* and *in vivo*. The enzastaurin-mediated reduction in proliferation has previously been demonstrated in a number of solid cancer models and myeloma cell lines.[47] Proliferating CLL cells are more prone to undergo clonal evolution, which can result in the development of detrimental chromosomal abnormalities including 17p deletions that target p53, rendering the cells insensitive to first-line therapies used for CLL.[48] Indeed, up-regulation of activation-induced deaminase has been associated with elevated double-strand DNA breaks in CLL cells, promoting the generation of genetic aberrations.[20] Therapies that reduce proliferation do, therefore, offer an important treatment option for progressive CLL. Our findings support the development of clinical studies with ruboxistaurin and sotrastaurin in CLL, given the recent promising data assessing the clinical efficacy of BCR-targeting inhibitors such as the Btk inhibitor ibrutinib.[49] In support of this, AEB071 is currently being studied in a phase II clinical trial in diffuse large B-cell lymphoma, and has recently been demonstrated to have pre-clinical activity in CLL *in vitro* and *in vivo*.[50] Targeting PKC, and in particular PKCβ, is especially pertinent given the recent findings of Lutzny *et al.*, who demonstrated that PKCβII expression in bone marrow stromal cells is essential for the survival and development of CLL cells.[51] Therefore, inhibition of PKCβ may modify the tumor microenvironment, which has been established to play a critical role in supporting CLL survival, proliferation and chemoresistance.[52]

Collectively, our results demonstrate the potential for therapeutic agents targeting PI3K/PKCβ–related signaling pathways, and highlight the translational applicability of the PKCα-KR mouse model as a pre-clinical model for the

development of poor prognostic CLL. Moreover, our mouse model provides a powerful tool for delineating the molecular events that occur downstream of PKCα subversion during the initiation of cellular transformation, enabling the identification of potential novel therapeutic targets for CLL.

Acknowledgments

The authors would like to thank Odette Middleton for critically reviewing the manuscript. This work was funded by an MRC new investigator research grant (Ref: G0601099), an MRC/AstraZeneca project grant (Ref: MR/K014854/1) and an LLR project grant (Ref. 13012). MV was supported by a Lady Tata Memorial Trust Award, AMMcC was supported by an MRC Clinical Research Training Fellowship and the flow cytometry facility was supported by KKLF (KKL501). We would like to thank Lilly and Co. for providing the enzastaurin.

Authorship and Disclosures

Information on authorship, contributions, and financial & other disclosures was provided by the authors and is available with the online version of this article at www.haematologica.org.

References

1. Dighiero G. CLL Biology and prognosis. Hematology Am Soc Hematol Educ Program. 2005:278-84.
2. Hanada M, Delia D, Aiello A, Stadtmauer E, Reed JC. bcl-2 gene hypomethylation and high-level expression in B-cell chronic lymphocytic leukemia. Blood. 1993;82(6):1820-1828.
3. Messmer BT, Messmer D, Allen SL, et al. In vivo measurements document the dynamic cellular kinetics of chronic lymphocytic leukemia B cells. J Clin Invest. 2005;115(3):755-764.
4. Ghia P, Chiorazzi N, Stamatopoulos K. Microenvironmental influences in chronic lymphocytic leukaemia: the role of antigen stimulation. J Intern Med. 2008;264(6):549-562.
5. Herishanu Y, Pérez-Galán P, Liu D, et al. The lymph node microenvironment promotes B-cell receptor signaling, NF-kappaB activation, and tumor proliferation in chronic lymphocytic leukemia. Blood. 2011;117(2):563-574.
6. Morilla A, Gonzalez de Castro D, Del Giudice I, et al. Combinations of ZAP-70, CD38 and IGHV mutational status as predictors of time to first treatment in CLL. Leuk Lymphoma. 2008;49(11):2108-2115.
7. Hamblin TJ, Davis Z, Gardiner A, Oscier DG, Stevenson FK. Unmutated Ig V(H) genes are associated with a more aggressive form of chronic lymphocytic leukemia. Blood. 1999;94(6):1848-1854.
8. Wiestner A, Rosenwald A, Barry TS, et al. ZAP-70 expression identifies a chronic lymphocytic leukemia subtype with unmutated immunoglobulin genes, inferior clinical outcome, and distinct gene expression profile. Blood. 2003;101(12):4944-4951.
9. Nakagawa R, Soh JW, Michie AM. Subversion of PKCα signaling in hematopoietic progenitor cells results in the generation of a B-CLL-like population in vivo. Cancer Res. 2006;66(1):527-534.
10. Bichi R, Shinton SA, Martin ES, et al. Human chronic lymphocytic leukemia modeled in mouse by targeted TCL1 expression. Proc Natl Acad Sci USA. 2002;99(10):6955-6960.
11. McCaig AM, Cosimo E, Leach MT, Michie AM. Dasatinib inhibits B cell receptor signalling in chronic lymphocytic leukaemia but novel combination approaches are required to overcome additional pro-survival microenvironmental signals. Br J Haematol. 2011;153(2):199-211.
12. Soh JW, Lee EH, Prywes R, Weinstein IB. Novel roles of specific isoforms of protein kinase C in activation of the c-fos serum response element. Mol Cell Biol. 1999; 19(2):1313-1324.
13. Nakagawa R, Mason SM, Michie AM. Determining the role of specific signaling molecules during lymphocyte development in vivo: instant transgenesis. Nat Protoc. 2006;1(3):1185.
14. Cosimo E, McCaig AM, Carter-Brzezinski LJ, et al. Inhibition of NF-κB-mediated signaling by the cyclin-dependent kinase inhibitor CR8 overcomes prosurvival stimuli to induce apoptosis in chronic lymphocytic leukemia cells. Clin Cancer Res. 2013;19(9): 2393-2405.
15. White HN. Restriction-PCR fingerprinting of the immunoglobulin VH repertoire: direct detection of an immune response and global analysis of B cell clonality. Eur J Immunol. 1998;28(10):3268-3279.
16. Nakagawa R, Vukovic M, Cosimo E, Michie AM. Modulation of PKC-α promotes lineage reprogramming of committed B lymphocytes. Eur J Immunol. 2012;42(4):1005-1015.
17. Fallah-Arani F, Schweighoffer E, Vanes L, Tybulewicz VL. Redundant role for Zap70 in B cell development and activation. Eur J Immunol. 2008;38(6):1721-1733.
18. Longo PG, Laurenti L, Gobessi S, Sica S, Leone G, Efremov DG. The Akt/Mcl-1 pathway plays a prominent role in mediating antiapoptotic signals downstream of the B-cell receptor in chronic lymphocytic leukemia B cells. Blood 2008;111(2):846-855.
19. Palacios F, Moreno P, Morande P, et al. High expression of AID and active class switch recombination might account for a more aggressive disease in unmutated CLL patients: link with an activated microenvironment in CLL disease. Blood. 2010;115 (22):4488-4496.
20. Patten PE, Chu CC, Albesiano E, et al. IGHV-unmutated and IGHV-mutated chronic lymphocytic leukemia cells produce activation-induced deaminase protein with a full range of biologic functions. Blood. 2012;120(24):4802-4811.
21. Abrams ST, Lakum T, Lin K, et al. B cell receptor signalling in chronic lymphocytic leukaemia cells is regulated by overexpressed active protein kinase C(beta)II. Blood. 2006;109(3):1193-1201.
22. Alkan S, Huang Q, Ergin M, et al. Survival role of protein kinase C (PKC) in chronic lymphocytic leukemia and determination of isoform expression pattern and genes altered by PKC inhibition. Am J Hematol. 2005;79(2):97-106.
23. Goode N, Hughes K, Woodgett JR, Parker PJ. Differential regulation of glycogen synthase kinase-3 beta by protein kinase C isotypes. J Biol Chem. 1992;267(24):16878-16882.
24. Griner EM, Kazanietz MG. Protein kinase C and other diacylglycerol effectors in cancer. Nat Rev Cancer. 2007;7(4):281-294.
25. Michie AM, Nakagawa R. The link between PKCa regulation and cellular transformation. Immunol Letts. 2005;96(2):155-162.
26. Tan M, Li P, Sun M, Yin G, Yu D. Upregulation and activation of PKC alpha by ErbB2 through Src promotes breast cancer cell invasion that can be blocked by combined treatment with PKC alpha and Src inhibitors. Oncogene. 2006;25(23):3286-3295.
27. Lønne GK, Cornmark L, Zahirovic IO, Landberg G, Jirström K, Larsson C. PKCalpha expression is a marker for breast cancer aggressiveness. Mol Cancer. 2010;9:76.
28. Alvaro V, Prevostel C, Joubert D, Slosberg E, Weinstein BI. Ectopic expression of a mutant form of PKCalpha originally found in human tumors: aberrant subcellular translocation and effects on growth control. Oncogene. 1997;14(6):677-685.
29. Neill GW, Ghali LR, Green JL, Ikram MS, Philpott MP, Quinn AG. Loss of protein kinase Calpha expression may enhance the tumorigenic potential of Gli1 in basal cell carcinoma. Cancer Res. 2003;63(15):4692-4697.
30. Tibudan SS, Wang Y, Denning MF. Activation of protein kinase C triggers irreversible cell cycle withdrawal in human keratinocytes. J Invest Dermatol. 2002;119(6): 1282-1289.
31. Detjen KM, Brembeck FH, Welzel M, et al. Activation of protein kinase Calpha inhibits growth of pancreatic cancer cells via p21(cip)-mediated G(1) arrest. J Cell Sci. 2000;113(Pt 17):3025-3035.
32. Gökmen-Polar Y, Murray NR, Velasco MA, Gatalica Z, Fields AP. Elevated protein kinase C betaII is an early promotive event in colon carcinogenesis. Cancer Res. 2001;61(4): 1375-1381.
33. Oster H, Leitges M. Protein kinase C alpha but not PKCzeta suppresses intestinal tumor formation in ApcMin/+ mice. Cancer Res. 2006;66(14):6955-6963.
34. Leitges M. Functional PKC in vivo analysis using deficient mouse models. Biochem Soc Trans. 2007;35(Pt 5):1018-1020.
35. Murray NR, Davidson LA, Chapkin RS, Clay Gustafson W, Schattenberg DG, Fields AP. Overexpression of protein kinase C betaII induces colonic hyperproliferation and increased sensitivity to colon carcinogenesis. J Cell Biol. 1999;145(4):699-711.
36. Holler C, Piñón JD, Denk U, et al. PKCbeta is essential for the development of chronic lymphocytic leukemia in the TCL1 transgenic mouse model: validation of PKCbeta as a therapeutic target in chronic lymphocyt-

ic leukemia. Blood 2009;113(12):2791-2794.
37. Leontieva OV, Black JD. Identification of two distinct pathways of protein kinase Calpha down-regulation in intestinal epithelial cells. J Biol Chem. 2004;279(7):5788-5801.
38. Blyth K, Morton JP, Sansom OJ. The right time, the right place: will targeting human cancer-associated mutations to the mouse provide the perfect preclinical model? Curr Opin Genet Dev. 2012;22(1):28-35.
39. Klein U, Lia M, Crespo M, et al. The DLEU2/miR-15a/16-1 cluster controls B cell proliferation and its deletion leads to chronic lymphocytic leukemia. Cancer Cell. 2010;17(1):28-40.
40. Johnson AJ, Lucas DM, Muthusamy N, et al. Characterization of the TCL-1 transgenic mouse as a preclinical drug development tool for human chronic lymphocytic leukemia. Blood. 2006;108(4):1334-1338.
41. Herling M, Patel KA, Khalili J, et al. TCL1 shows a regulated expression pattern in chronic lymphocytic leukemia that correlates with molecular subtypes and proliferative state. Leukemia. 2006;20(2):280-285.
42. Fais F, Ghiotto F, Hashimoto S, et al. Chronic lymphocytic leukemia B cells express restricted sets of mutated and unmutated antigen receptors. J Clin Invest. 1998;102 (8):1515-1525.
43. Yan XJ, Albesiano E, Zanesi N, et al. B cell receptors in TCL1 transgenic mice resemble those of aggressive, treatment-resistant human chronic lymphocytic leukemia. Proc Natl Acad Sci USA. 2006;103(31):11713-11718.
44. Gobessi S, Belfiore F, Bennardo S, Doe B, Laurenti L, Efremov DG. Expression of ZAP-70 does not accelerate leukemia development and progression in the Eμ-TCL1 transgenic mouse model of chronic lymphocytic leukemia. 54th ASH Annual Meeting Abstract 2012;641:925.
45. Liffraud C, Quillet-Mary A, Fournié JJ, Laurent G, Ysebaert L. Protein phosphatase-2A activation is a critical step for enzastaurin activity in chronic lymphoid leukemia cells. Leuk Lymphoma 2012;53(5):966-972.
46. Negro R, Gobessi S, Longo PG, et al. Overexpression of the autoimmunity-associated phosphatase PTPN22 promotes survival of antigen-stimulated CLL cells by selectively activating AKT. Blood. 2012;119 (26):6278-6287.
47. Neri A, Marmiroli S, Tassone P, et al. The oral protein-kinase C beta inhibitor enzastaurin (LY317615) suppresses signalling through the AKT pathway, inhibits proliferation and induces apoptosis in multiple myeloma cell lines. Leuk Lymphoma. 2008;49(7):1374-1383.
48. Stilgenbauer S, Sander S, Bullinger L, et al. Clonal evolution in chronic lymphocytic leukemia: acquisition of high-risk genomic aberrations associated with unmutated VH, resistance to therapy, and short survival. Haematologica 2007;92(9):1242-1245.
49. Byrd JC, Furman RR, Coutre SE, et al. Targeting BTK with ibrutinib in relapsed chronic lymphocytic leukemia. N Engl J Med. 2013;369(1):32-42.
50. El-Gamal D, Williams K, LaFollette TD, et al. PKC-β as a therapeutic target in CLL: PKC inhibitor AEB071 demonstrates preclinical activity in CLL. Blood 2014;124(9):1481-1491.
51. Lutzny G, Kocher T, Schmidt-Supprian M, et al. Protein kinase C-β-dependent activation of NF-κB in stromal cells is indispensable for the survival of chronic lymphocytic leukemia B Cells in vivo. Cancer Cell. 2013; 23(1):77-92.
52. Ten Hacken E, Burger J. Molecular pathways: targeting the microenvironment in chronic lymphocytic leukemia- focus on the B cell receptor. Clin Cancer Res. 2014;20 (3):548-556.